

Row orientation and viewing geometry effects on row-structured vine crops for chlorophyll content estimation

F. Meggio, P.J. Zarco-Tejada, J.R. Miller, P. Martín, M.R. González, and A. Berjón

Abstract. Methods for chlorophyll $a + b$ (C_{ab}) estimation in row-structured crops that account for row orientation and sun geometry are presented in this research. Airborne campaigns provided imagery over a total of 72 study sites from 14 *Vitis vinifera* L. fields with the Compact Airborne Spectrographic Imager (CASI) hyperspectral sensor in different sun geometries and a wide range of row orientations. Two different CASI acquisition modes were used, comprising 1 and 4 m spatial resolutions with 8 and 72 bands, respectively, in the visible and near-infrared spectral regions. Airborne campaigns were acquired over the same sites in the morning and in the afternoon to assess the bidirectional reflectance distribution function (BRDF) effects on the imagery owing to the different fractions of shadow as a function of the sun viewing geometries and the row orientation. Narrow-band indices sensitive to chlorophyll content (TCARI/OSAVI (transformed chlorophyll absorption in reflectance index / optimized soil-adjusted vegetation index)) and canopy structure (normalized difference vegetation index (NDVI)) were calculated from the CASI imagery. The effects on the canopy reflectance of different sun viewing geometries and row orientation were studied through a modelling approach. The validity of narrow-band indices for C_{ab} content estimation at the canopy level was assessed using an upscaling approach with the Markov-chain canopy reflectance model (MCRM), with additions to simulate the row crop structure (rowMCRM) to account for the effects of vineyard structure, vine dimensions, row orientation, and soil and shadow effects on the canopy reflectance. Several predictive algorithms were tested in this study to explore the importance of row orientation and viewing geometry of row-structured crops. New predictive relationships were developed with the rowMCRM model between C_{ab} and TCARI/OSAVI as a function of structural properties of the canopy, taking into account diurnal variations in the viewing geometry and row orientation. One of these new predictive algorithms for C_{ab} content estimation, valid for a typical range of viewing geometries and row orientations, was successfully applied to the 72 study areas, yielding an RMSE in leaf chlorophyll content estimation of 10.2 and 10.6 $\mu\text{g}\cdot\text{cm}^{-2}$ for morning and afternoon sun geometries, respectively.

Résumé. Dans cette recherche, on présente des méthodes d'estimation de la chlorophylle $a + b$ (C_{ab}) pour les cultures en rang qui tiennent compte de l'orientation des rangs et de la géométrie visée/soleil. Des images ont été acquises au-dessus de 72 sites d'étude répartis sur 14 champs de *Vitis vinifera* L. lors de campagnes aéroportées à l'aide du capteur hyperspectral CASI (« Compact Airborne Spectrographic Imager ») dans différentes géométries de visée/soleil et pour diverses orientations de rangs. Deux modes d'acquisition différents du CASI ont été utilisés, comprenant les résolutions spatiales de 1 m et de 4 m, avec 8 et 72 bandes respectivement, dans la région spectrale du visible et du proche infrarouge. Des campagnes d'acquisition aéroportées ont été réalisées au-dessus des mêmes sites durant la matinée et en après-midi pour évaluer les effets de la réflectance bidirectionnelle (FDRB) sur les images dus aux différentes fractions d'ombre en fonction des géométries de visée/soleil et de l'orientation des rangs. Les indices en bande étroite sensibles à la teneur en chlorophylle (TCARI/OSAVI (« transformed chlorophyll absorption in reflectance index / optimized soil-adjusted vegetation index »)) ainsi qu'à la structure du couvert (« normalized difference vegetation index » (NDVI)) ont été calculés à l'aide des images du CASI. Les effets de différentes géométries de visée/soleil et de l'orientation des rangs sur la réflectance du couvert ont été étudiés par le biais d'une approche de modélisation. La validité des indices en bande étroite pour l'estimation de la

Received 20 December 2007. Accepted 7 April 2008. Published on the *Canadian Journal of Remote Sensing* Web site at <http://pubs.nrc-cnrc.gc.ca/cjrs> on 29 August 2008.

F. Meggio. University of Padova, Department of Environmental Agronomy and Crop Science, Viale dell'Università 16, I-35020 Legnaro (Padova), Italy.

P.J. Zarco-Tejada¹. Instituto de Agricultura Sostenible (IAS), Consejo Superior de Investigaciones Científicas (CSIC), Alameda del Obispo, s/n, 14004 – Córdoba, Spain.

J.R. Miller. Department of Earth and Space Science and Engineering, York University, 4700 Keele Street, Toronto, ON M3J 1P3, Canada.

P. Martín and M.R. González. Departamento de Producción Vegetal y Recursos Forestales, Universidad de Valladolid, 34004 Palencia, Spain.

A. Berjón. Departamento de Física Teórica, Atómica y Óptica, Universidad de Valladolid, 47005 Valladolid, Spain.

¹Corresponding author (e-mail: pzarco@ias.csic.es).

teneur en C_{ab} au niveau du couvert a été évaluée à l'aide d'une approche de mise à l'échelle supérieure avec le modèle MCRM (« Markov-chain canopy reflectance model »), avec des ajouts pour simuler la structure des rangs des cultures (rowMCRM) afin de tenir compte des effets de la structure du vignoble, de la dimension des vignes, de l'orientation des rangs et des effets du sol et des ombres sur la réflectance du couvert. Plusieurs algorithmes prédictifs ont été testés dans cette étude pour examiner l'importance de l'orientation des rangs et de la géométrie de visée dans les cultures en rangs. De nouvelles relations prédictives ont été développées entre C_{ab} et TCARI/OSAVI avec le modèle rowMCRM en fonction des propriétés structurelles du couvert, prenant en considération les variations diurnes de la géométrie de visée et l'orientation des rangs. Un de ces nouveaux algorithmes prédictifs pour l'estimation de C_{ab} , valide pour des géométries de visée et des orientations de rangs caractéristiques, a été appliqué avec succès aux 72 zones d'étude, donnant des valeurs de RMSE respectivement de 10,2 et 10,6 $\mu\text{g}\cdot\text{cm}^{-2}$ pour les géométries visée/soleil du matin et de l'après-midi pour l'estimation de la teneur en chlorophylle des feuilles.

[Traduit par la Rédaction]

Introduction

Estimation of leaf biochemical constituents in row-structured crop canopies requires appropriate modelling methods to account for row orientation and sun geometry, which affect the proportions of shadows, sunlit and shaded soil, and pure vegetation scene components (Zarco-Tejada et al., 2005). Previous studies assessing within-field variability in precision viticulture highlighted the potential of remote sensing methods to estimate variations in some biophysical and structural parameters (Hall et al., 2002; 2003). These new precision farming techniques aim at delineating homogeneous management zones based on remotely sensed biophysical variable estimates. In particular, within-field variability detection in vineyards would enable the generation of maps with a gradient of management zones potentially linked to wine quality (Johnson et al., 2001). In this context, such research objectives were explored using high spatial resolution hyperspectral remote sensing imagery and physical methods to estimate leaf biochemical constituents as a means to assess within-field vine status and function (Zarco-Tejada et al., 2005).

One of the most important biochemical constituents for understanding plant functioning and photosynthetic status is leaf chlorophyll *a* + *b* concentration (C_{ab}), which can be detected by photosynthetic pigment responses in leaf reflectance in the green peak and along the red-edge spectral region (Rock et al., 1988; Vogelmann et al., 1993; Carter, 1994; Gitelson and Merzlyak, 1996). The estimation of chlorophyll concentration on crop and forest species at canopy scales has been assessed with success using new narrow-band optical indices and physical methods (a full review of indices can be found in Zarco-Tejada et al. (2005)) calculated from hyperspectral reflectance data (Haboudane et al., 2002; 2004; Zarco-Tejada et al., 2001). Red-edge reflectance indices, spectral and derivative indices, and derivative ratios have demonstrated a good sensitivity for C_{ab} estimation from canopy reflectance using airborne hyperspectral data. Recently, combinations of indices, based on the transformed chlorophyll absorption in reflectance index (TCARI) (Haboudane et al., 2002), the modified chlorophyll absorption in reflectance index (MCARI) (Daughtry et al., 2000), and the optimized soil-

adjusted vegetation index (OSAVI) (Rondeaux et al., 1996), such as TCARI/OSAVI and MCARI/OSAVI, have been demonstrated to successfully minimize soil background and leaf area index (LAI) variation in crops. These narrow-band indices linked to radiative transfer simulations provided predictive relationships for precision agriculture applications with hyperspectral imagery in continuous crop canopies (Haboudane et al., 2002), and have been adapted to open-tree canopy orchards (Zarco-Tejada et al., 2004).

Although successful results were obtained for biochemical constituent estimation at the canopy level in homogeneous closed-canopy crops (Haboudane et al., 2004), airborne remote sensing and unmanned aerial vehicle platforms require predictive algorithms insensitive to the large bidirectional reflectance distribution function (BRDF) effects caused by row orientations and sun geometries. Manned and unmanned aerial vehicle (UAV) platforms for precision agriculture applications are operationally able to acquire imagery within a wide range of sun angle conditions, generating imagery under very different viewing geometries. In addition, the predictive algorithms used for parameter estimation are generally developed for a given set of viewing conditions and crop structural characteristics. In particular, algorithms developed for closed canopies (i.e., corn, wheat) may not be valid for open-canopy orchards and row-structured canopies (i.e., vineyards). Differences in row-crop structural parameters, such as row height, row width, row LAI, varying soil backgrounds, and visible soil proportion, were assessed using hyperspectral imagery (Zarco-Tejada et al., 2005) to demonstrate their important effects on canopy reflectance, and therefore in estimation of C_{ab} . In addition, different sun viewing geometries (i.e., sun azimuth and zenith angles) may have a greater influence on the optical vegetation index and the estimated leaf biochemical constituent in row-structured canopies. This is due to the diurnal variations in amount and proportion of shadows that affect canopy reflectance as a function of the BRDF. Moreover, algorithms developed for a given combination of row orientation and (or) sun angle may not be valid for different conditions (i.e., morning and (or) afternoon viewing geometries or north-south and east-west row orientations). It is important, therefore, that successful leaf-level indices are investigated at

the canopy level through upscaling simulations with appropriate physical methods and very high spatial resolution accounting for BRDF effects.

This research further develops previous work (Zarco-Tejada et al., 2005), advancing the assessment of the optical properties of *Vitis vinifera* L. for C_{ab} estimation over a wider range of conditions using narrow-band indices and radiative transfer models. Specific leaf optical indices are proposed for upscaling simulation with the Markov-chain canopy reflectance model (MCRM) (Kuusk, 1995a; 1995b) with additions to simulate the row crop structure (rowMCRM). The linked PROSPECT–rowMCRM is used to model vineyard scene component proportions, row orientations, sun viewing geometries, vineyard dimensions, and background effects with high spatial resolution hyperspectral airborne imagery. The main focus is on modelling the row orientation and sun geometries in a row-structured canopy to develop a new algorithm for C_{ab} estimation in the context of precision agriculture.

Methods

Study site description

The data acquisition campaigns were conducted in July 2003 in Northern Spain. A total of 14 full production vineyards, located in the western area of Ribera del Duero Apellation d'Origine at an altitude of about 800 m above sea level, were selected for sampling collections. Data collection comprised a total of 72 study sites, with each vineyard including at least 4 study areas of 10 m × 10 m in size. The study sites used for ground and airborne collections were based on a plot network currently monitored by the local government, with specific sites selected to assure that an appropriate variability in leaf biochemistry and vine physiological conditions would be found across the sites. All vineyards correspond to cv. Tempranillo grafted on 110-Richter rootstock, with ages ranging between 7 and 16 years. Vine densities ranged between 2200 and 4000 vines per hectare, and plants were trained to a simple or double Cordon Royat system (as described in detail in Martin et al. (2007)). The vineyards differ in canopy structure, soil background, and planting row orientation ranged from 0° to 180° N, with row direction angle measured clockwise from north.

Airborne campaigns with CASI hyperspectral sensor to acquire BRDF datasets

The Compact Airborne Spectrographic Imager (CASI) sensor was flown over Spain in collaboration with York University, Canada, and the Instituto Nacional de Tecnica Aeroespacial, Spain. The CASI imagery was collected on two airborne missions, each with a specific sensor mode of operation: (i) the Mapping Mission (spatial mode), with 1 m spatial resolution and 8 user-selected spectral bands placed in the spectrum to enable the calculation of specific narrow-band indices sensitive to pigment concentration (bands were centred at 490, 550, 670, 700, 750, 762, 775, and 800 nm with full-

width at half-maximum ranging between 7 and 12 nm); and (ii) the Hyperspectral Mission (spectral mode), with 4 m spatial resolution and 72 channels at 7.5 nm spectral resolution. The 12-bit radiometric resolution data collected by CASI were processed to at-sensor radiance using calibration coefficients derived in the laboratory by the Earth Observation Laboratory (EOL), York University, Canada. Aerosol optical depth data were collected at 340, 380, 440, 500, 670, 870, and 1200 nm using a Microtops II sunphotometer (Solar Light Co., Philadelphia, Pennsylvania, USA) in the same study area and at the same time of data acquisition to derive aerosol optical depth (AOD) at 550 nm. Atmospheric correction was applied to CASI imagery using the CAM5S atmospheric correction model (O'Neill et al., 1997). Global positioning system (GPS) data collected onboard the aircraft were used for the geocoding and image registration. Soil reflectance spectra measured for each site at ground level were used to perform a flat-field correction (Ben-Dor and Levin, 2000) to the CASI reflectance spectra that compensated for residual effects on derived surface reflectance estimations in the atmospheric water and oxygen absorption spectral regions. BRDF effects due to sun geometry combined with the vine row directions were captured by flying all study sites in the morning (9:30–11:30 AM) and in the afternoon (2:30–4:00 PM). Both datasets were acquired with band centres and bandwidths that enabled the calculation of vegetation indices sensitive to chlorophyll concentration, such as TCARI/OSAVI (Haboudane et al., 2002):

$$TCARI/OSAVI = \frac{3[(R_{700} - R_{670}) - 0.2(R_{700} - R_{550})(R_{700} / R_{670})]}{(1 + 0.16)(R_{800} - R_{670}) / (R_{800} + R_{670} + 0.16)} \quad (1)$$

Vine structural measurements and leaf sampling for biochemical determination

Concurrent with the airborne missions, field sampling campaigns were conducted to enable biochemical analysis of leaf C_{ab} as well as to measure leaf reflectance (R) and leaf transmittance (T) to assess the vineyard leaf optical properties. Each 10 m × 10 m study area was used to collect 80 leaves, 50 of which were used for determination of dry matter, nitrogen (N), phosphorus (P), potassium (K), calcium (Ca), magnesium (Mg), and iron (Fe) contents. A total of 20 leaves per site were collected for C_{ab} determination, and the leaf optical properties were measured on 10 leaves per site. Leaves used for determination of the optical properties were taken to the laboratory, and R and T measurements were made on the same day to avoid pigment degradation. Dry matter was measured by placing the samples in a preheated oven at 40 °C until a stable dry weight was reached. Canopy structural parameters determined on each study site consisted of grid size, number of vines within the 10 m × 10 m site, trunk height, plant height and width, and row orientation. Soil samples were collected at each site for laboratory chemical analysis. Foliar sampling was conducted from the top of the canopy on fully expanded leaves. Leaf R , T , and pigment determination were assessed following the protocol specified in Zarco-Tejada et al. (2005).

Table 1. Nominal values and ranges for parameters used for canopy simulation with rowMCRM for the vine study sites.

	Nominal values and range
Leaf parameters	
Chlorophyll $a + b$ (C_{ab})	20–90 $\mu\text{g}\cdot\text{cm}^{-2}$
Dry matter (C_m)	0.0035 $\text{mg}\cdot\text{cm}^{-2}$
Equivalent water thickness (C_w)	0.025 $\text{mg}\cdot\text{cm}^{-2}$
Structural parameter (N)	1.62
Canopy layer and structure parameters	
Row leaf area index (LAI)	1–5
Leaf angle distribution function (LADF)	$\epsilon = 0.95$; $\theta_n = 45^\circ$ (plagiophile)
Relative size (h_s)	0.083
Markov parameter (λ_z)	1.1
Leaf transmittance coefficient (t)	0.9
Leaf hair index (I_h)	0.1
Canopy height (C_H)	1.2–1.8 m
Crown width (C_W)	0.6–1.3 m
Visible soil strip length (leaf transmittance coefficient (V_s))	1.7–2.3 m
Difference between sun azimuth and row orientation (ψ)	4° – 245°
Background and viewing geometry	
Soil reflectance (ρ_s)	Specific for each site
Angstrom turbidity factor (β)	0.18
Sun azimuth angle	97° – 250°
Sun zenith angle (θ)	28° – 66°

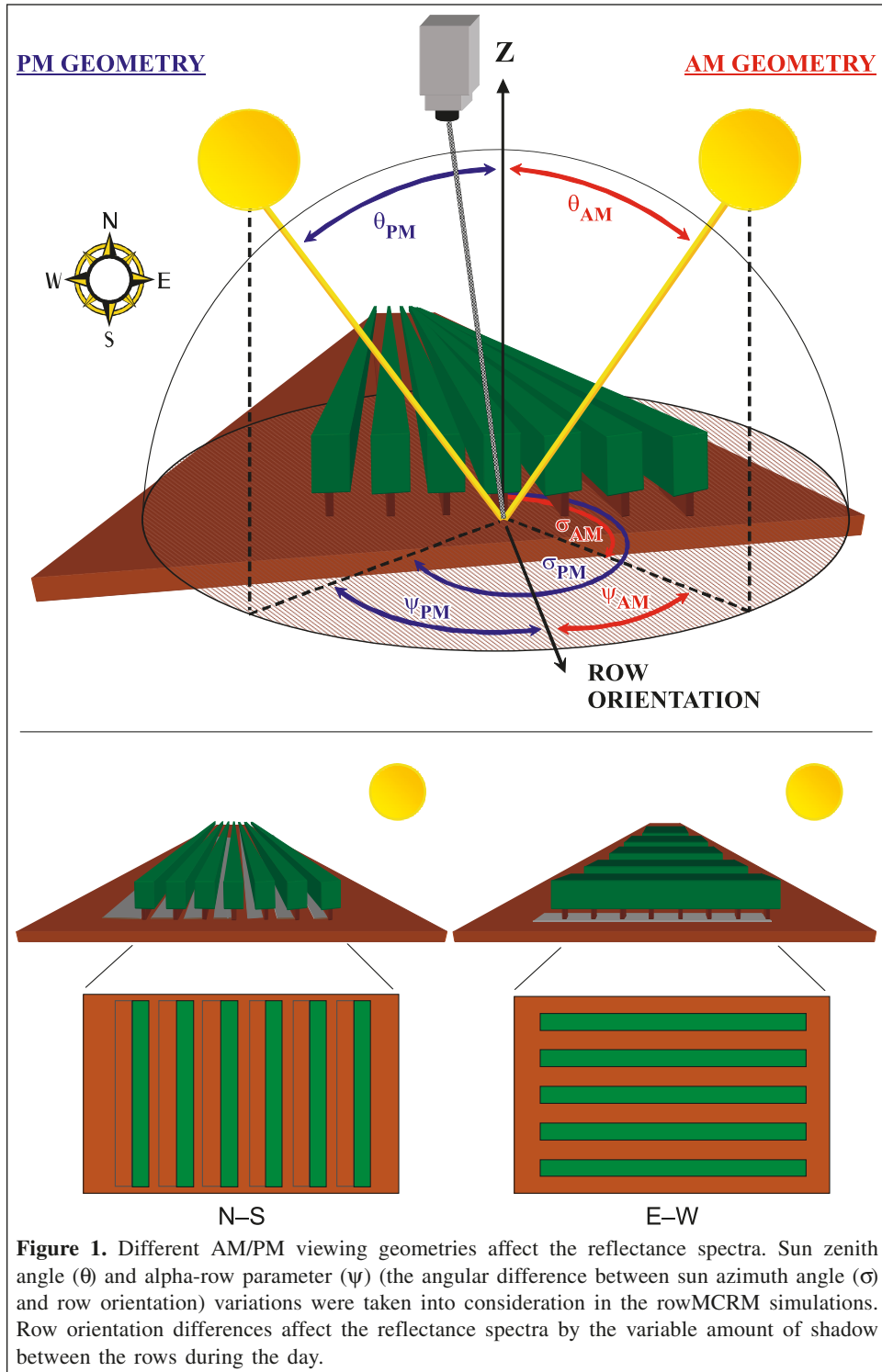
Assessment of BRDF and row orientation effects on canopy reflectance and TCARI/OSAVI with the rowMCRM canopy model

The MCRM (Kuusk, 1995a; 1995b) with additions to simulate the row crop structure (described in detail in Zarco-Tejada et al. (2005)) was considered an optimum choice to access BRDF and row orientation effects on canopy reflectance and the leaf chlorophyll-sensitive index TCARI/OSAVI. The inputs required for the rowMCRM used in this study are shown in **Table 1**. These were the same nominal ranges of parameters defining leaf optical properties, canopy layer and structure, and soil background, as proposed in Zarco-Tejada et al. (2005). In addition, to assess the effects of BRDF and row orientation on canopy reflectance and the TCARI/OSAVI index, attention was focused on viewing-geometry parameters, such as sun azimuth (σ), sun zenith (θ), and row orientation angles (**Table 1**). **Figure 1** shows the large effects caused by shadows as a function of the sun angle and row orientation for two extreme conditions, representing morning (AM) and afternoon (PM) sun angles, and north–south and east–west row orientations. The ranges used in the model simulations were chosen to enhance the row orientation and viewing geometry variability between the different sites (**Figure 2**) for the two missions. Sun azimuth and row orientation angles are linked in the model by the alpha-row parameter (ψ), calculated as the angular difference between sun azimuth and row orientation, both of which were measured in a clockwise direction from north.

Results

BRDF effects on canopy reflectance: optical indices comparison

In this section, results are presented for the comparison between the analysis of reflectance spectra obtained from CASI images (**Figure 2**) and the simulations performed with the rowMCRM canopy model (**Table 1**). Reflectance spectra comparisons between AM and PM viewing geometries for all 14 vineyards showed an evident ($\%R$) offset along the entire spectrum from the visible through the near-infrared (NIR) wavelengths (**Figure 3a**). The observed reflectance amplitude offset for all the study sites between AM and PM datasets showed a higher spectral reflectance for all the wavelengths in the afternoon imagery relative to the spectra collected in the morning for the same sites. This effect was shown to be consistent with model simulations performed with the rowMCRM canopy reflectance model (**Figure 3b**). Simulations were conducted using input parameters specific for each site as measured in the field, assessing imagery-observed and model-simulated offsets. These simulations were performed for all the sites and showed consistent results for CASI datasets acquired in the morning and the afternoon. Results obtained for two narrow-band optical indices, the normalized difference vegetation index (NDVI) and TCARI/OSAVI, calculated from CASI reflectance spectra for each 10 m \times 10 m study area (comprising mixed vegetation–soil pixels) showed the BRDF effects on the indices (**Figure 4**).



In particular, the NDVI showed a good correlation between AM and PM datasets ($R = 0.9$, linear), with lower values obtained at the higher NDVI range (>0.35) from the PM dataset. TCARI/OSAVI, considered the best optical index for C_{ab} estimation in *V. vinifera* L. (Zarco-Tejada et al., 2005), has been shown to be more affected by BRDF effects ($R = 0.7$, linear), with higher values retrieved from the PM reflectance spectra.

RowMCRM simulations to assess BRDF effect as a function of vine row orientation and viewing geometry

Simulations conducted with the rowMCRM canopy reflectance model were performed to understand the importance of variations in viewing geometries and row orientation. In particular, different ranges of the alpha-row parameter were tested in terms of daily sun variations in

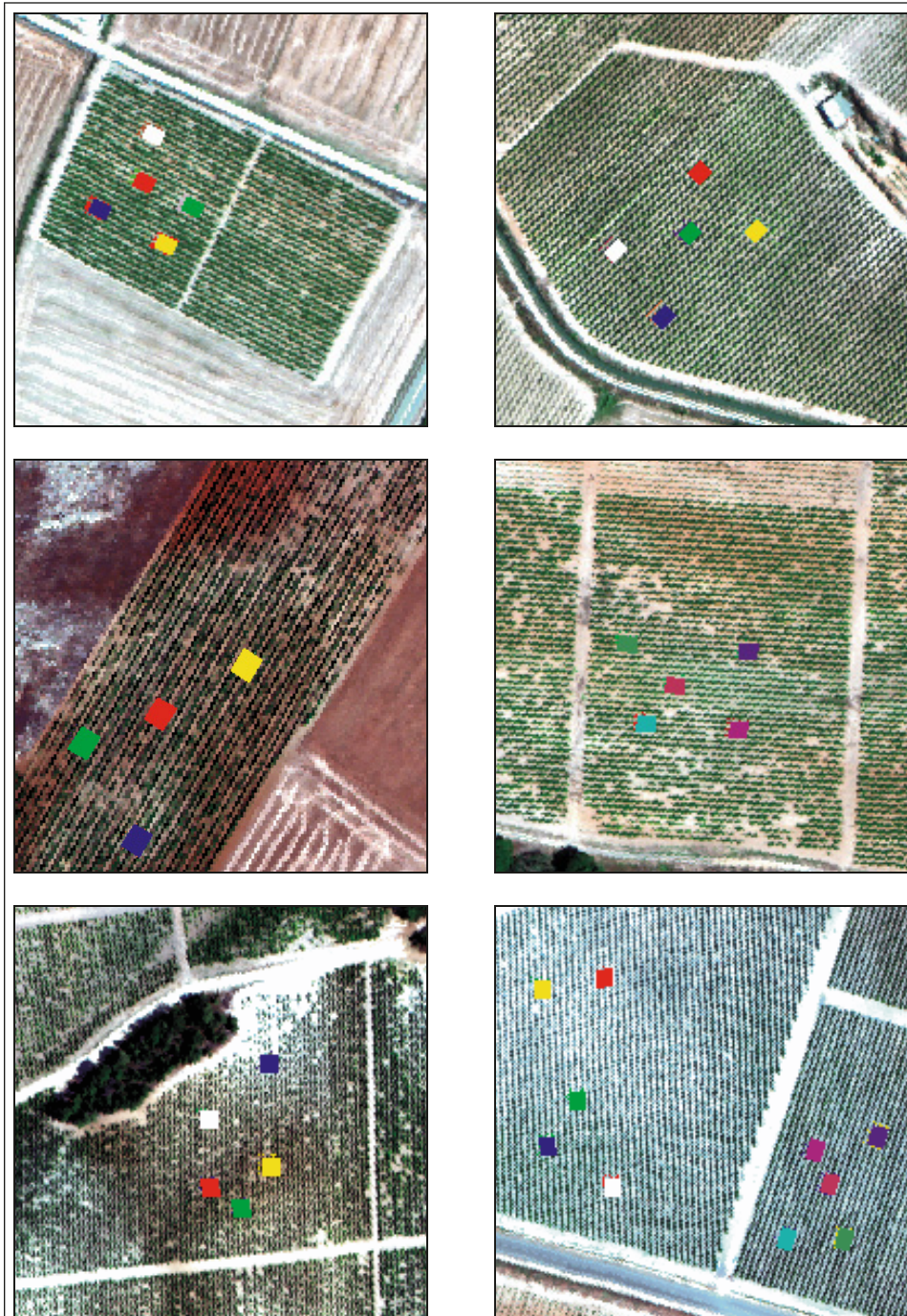


Figure 2. Airborne hyperspectral CASI-spatial mode (1 m spatial resolution) images. Different vineyards showed a heterogeneity of row orientations that with the varying viewing geometries during the day affected the reflectance spectrum.

azimuth and zenith angles, for different row orientations (**Table 1**). The most critical canopy model inputs for TCARI/OSAVI variation were tested by considering different ranges of viewing geometry and row orientation, such as row LAI, vine width and height, visible soil strip, chlorophyll content, and soil background. Mean vine dimensions in terms of vine height (1.2, 1.5, 1.8 m) and vine width (0.6, 1, 1.3 m) were used for all simulations.

The effects on TCARI/OSAVI as a function of different daily viewing geometries and row orientations (alpha-row, sun zenith angle) conditions (**Figure 5**) show the effects of differences in vine row LAI, with LAI = 1 (**Figure 5a**) and LAI = 5 (**Figure 5b**), considering also a different range of visible soil strip widths between 1.7 and 2.3 m. The alpha-row effect on TCARI/OSAVI during the day varies as a function of changing sun zenith angle, from 10° at midday to 60° in the early

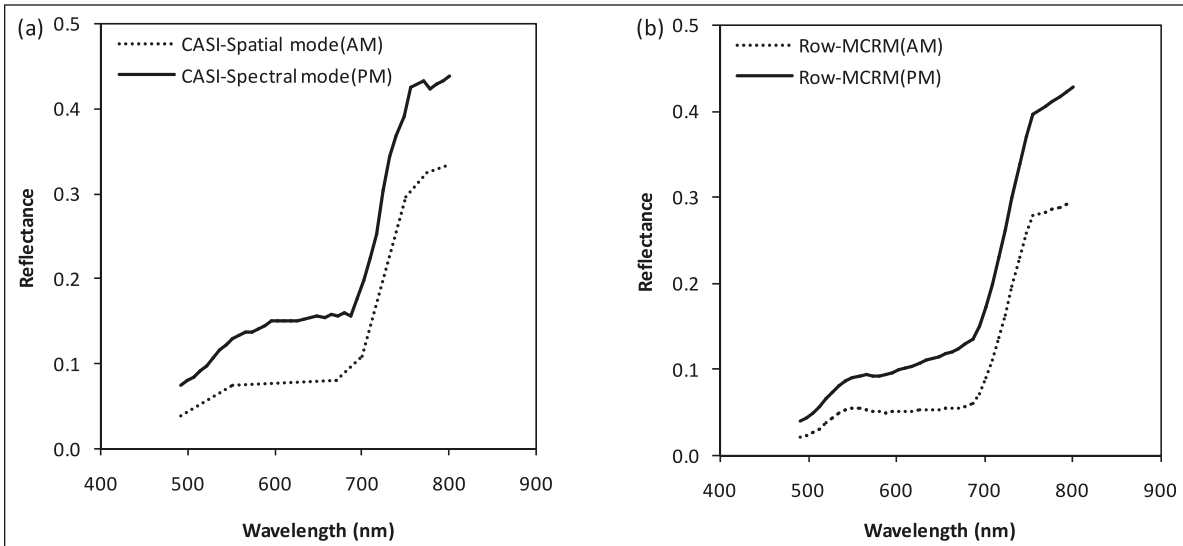


Figure 3. Spectra obtained for mixed vegetation–soil pixels: (i) CASI image spectra collected with the spatial mode (AM) and with the spectral mode (PM) (a); (ii) canopy reflectance spectra simulation conducted with rowMCRM as a function of alpha-row and sun zenith between AM and PM (b).

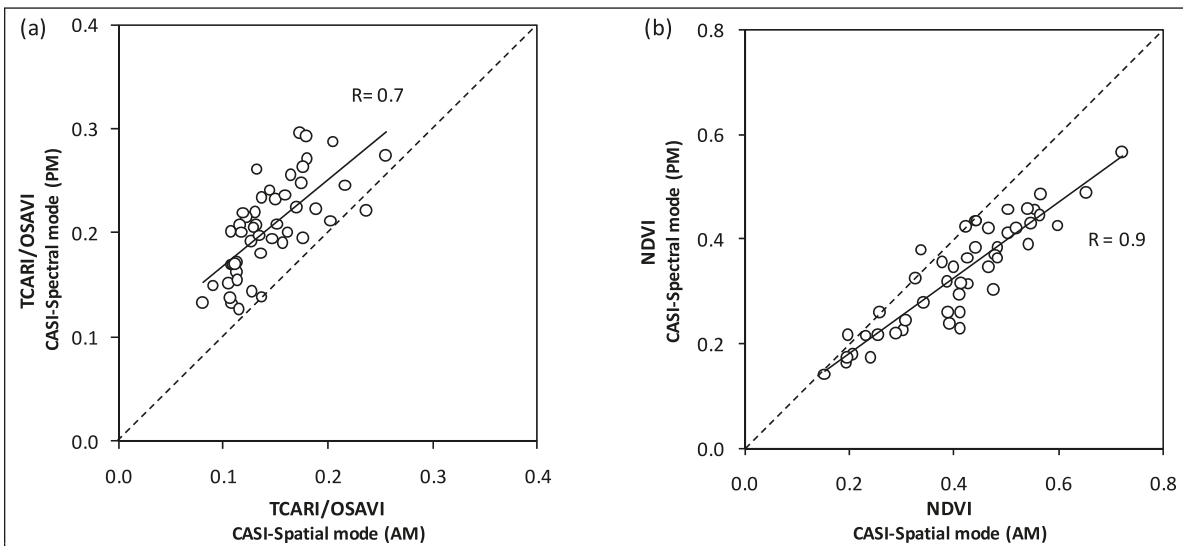
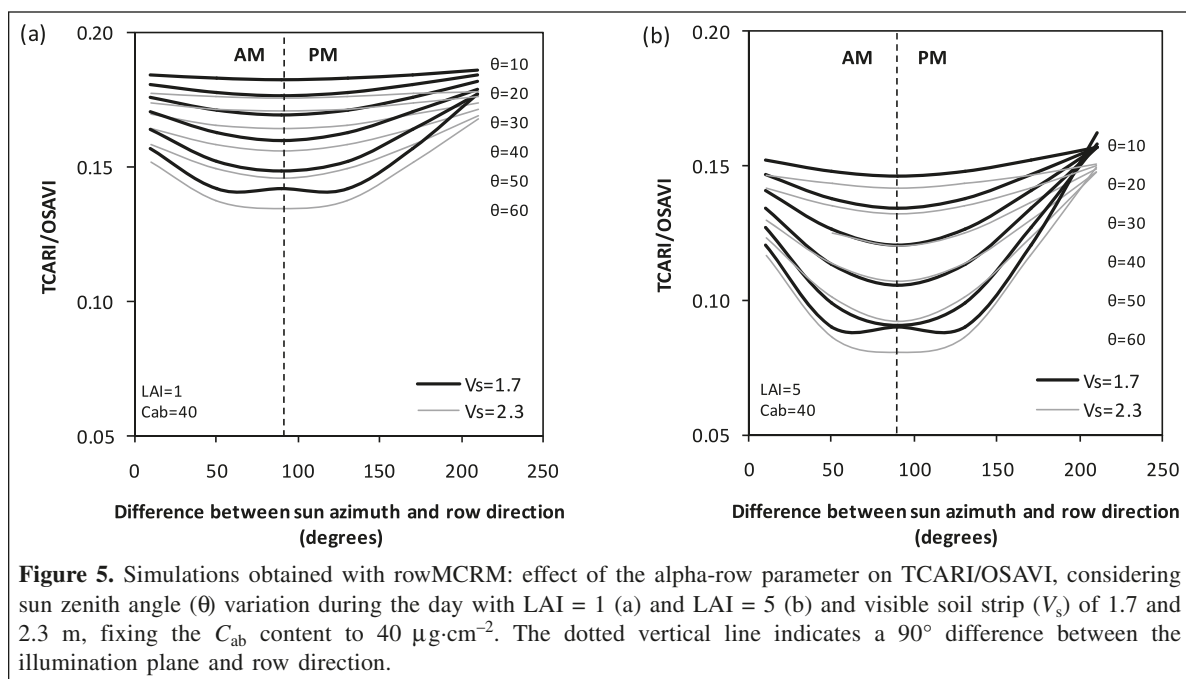


Figure 4. Relationships obtained for TCARI/OSAVI (a) and NDVI (b) calculated from CASI reflectance spectra between AM and PM, showing the BRDF effect on both indices. Linear relationships for AM and PM solar viewing geometries are shown: $R = 0.7$ for TCARI/OSAVI; $R = 0.9$ for NDVI.

morning–late afternoon. BRDF effects are minimized during midday hours due to the lower shadow content in the canopy pixel, resulting in a smaller influence on the canopy reflectance. BRDF effects are increased with higher row LAI and with higher visible soil strip length, which is minimized in the central part of the day. The analysis of canopy reflectance changes at different alpha-row conditions is complex due to the combined effects of the angular differences between row orientation and sun azimuth angle, parameters that vary independently. For this reason, the simulations were made by alternately fixing and varying both the row orientation and sun azimuth (Figure 5). Row orientation and sun azimuth angles

were varied as a function of time of day, using a range between 0° and 90° for morning geometry, and an afternoon range from 90° to 250° (Figure 5). Different ranges for sun zenith angle and alpha-row parameters enable the minimization of BRDF effects on the TCARI/OSAVI.

Soil background contributes greatly to TCARI/OSAVI as a function of different alpha-row conditions (Figure 6). A range of different soil background spectra (bright, medium, dark) collected during the field campaign (Zarco-Tejada et al., 2005) were tested in simulations for different viewing geometries at mid-AM and mid-PM ($\sigma = 30^\circ$) (Figure 6, left column) and early AM and late PM ($\sigma = 60^\circ$) (Figure 6, right column)



conditions in terms of sun zenith and alpha-row angles. Soil background affected TCARI/OSAVI as a function of the alpha-row angle more than that due to the different conditions of the visible soil strip. Again, row LAI effects on the index were higher at large solar azimuth angles than in the central part of the day. Alpha-row angle variations were studied for the relationship TCARI/OSAVI versus C_{ab} content (Figure 7) with different soil backgrounds (bright (Figure 7, top), medium (Figure 7, middle), and dark (Figure 7, bottom)), considering visible soil strip and row LAI (left–right) conditions. These simulations suggested low effects of row LAI on TCARI/OSAVI as a function of C_{ab} in vineyards relative to the larger effect of the visible soil strip due to different soil background brightness conditions.

Estimation of C_{ab} by upscaling relations obtained by rowMCRM simulations

The upscaling predictive relationships presented in Zarco-Tejada et al. (2005) were obtained only from the AM spatial-mode dataset for each field study site. These described the relationship between leaf C_{ab} and the TCARI/OSAVI using a range of LAI values between 1 and 5, for C_{ab} between 5 and 95 $\mu\text{g}\cdot\text{cm}^{-2}$. The remaining leaf parameters were fixed to values estimated by model inversion from leaf samples, with field structural measurements describing the vineyard canopy structure on each study site (Zarco-Tejada et al., 2005). The new simulations conducted in this study with the rowMCRM canopy model enabled the calculation of different predictive relationships, considering ranges for all input parameters (Table 1) for both AM and PM viewing geometry conditions and different row orientations. The simulations integrated ranges for leaf, structure, and soil background parameters with different viewing geometries. The differences between

different upscaling relationships obtained with rowMCRM simulations are shown in Figure 8. A simple simulation was undertaken by changing LAI and C_{ab} values only (Figure 8a) while fixing the remaining structural and background parameters and considering only an AM viewing geometry. A comprehensive iterative simulation was performed, varying all the input parameters (Figure 8b). In this case, all the TCARI/OSAVI estimates are not aligned along a curve but instead form a dispersed cloud around the fitting curve in response to the strong effect of soil background, LAI, visible strip, vine height and width, and the influence of daily differences in the viewing geometry and row orientation.

Different predictive algorithms were tested in this study (Table 2; Figure 9) to explore the importance of row orientation and viewing geometry of row-structured crops. In particular, we calculated the root mean square error (RMSE) between the C_{ab} measured in the field and the C_{ab} estimated by upscaling TCARI/OSAVI (calculated from CASI images for both AM and PM datasets) using published predictive algorithms (Zarco-Tejada, et al., 2005; Haboudane et al., 2002) and new predictive relationships presented in this study (Table 2). We observe that the RMSE between C_{ab} measured in the field and C_{ab} estimated using the upscaling relation proposed by Haboudane et al. (2002) (Table 2; Equation (1)) for closed corn canopies generates a poor result with a general overestimation of the C_{ab} content for both AM and PM datasets, with an RMSE of 41.2 and 32.9 $\mu\text{g}\cdot\text{cm}^{-2}$ for AM and PM datasets, respectively (Figure 9A). This shows clearly the importance of using an open-canopy model such as rowMCRM. When the relationship proposed by Zarco-Tejada et al. (2005) for open canopy and AM geometry was used (Table 2; Equation (2)), a much improved RMSE of 11.2 $\mu\text{g}\cdot\text{cm}^{-2}$ was obtained as expected, but not for the PM

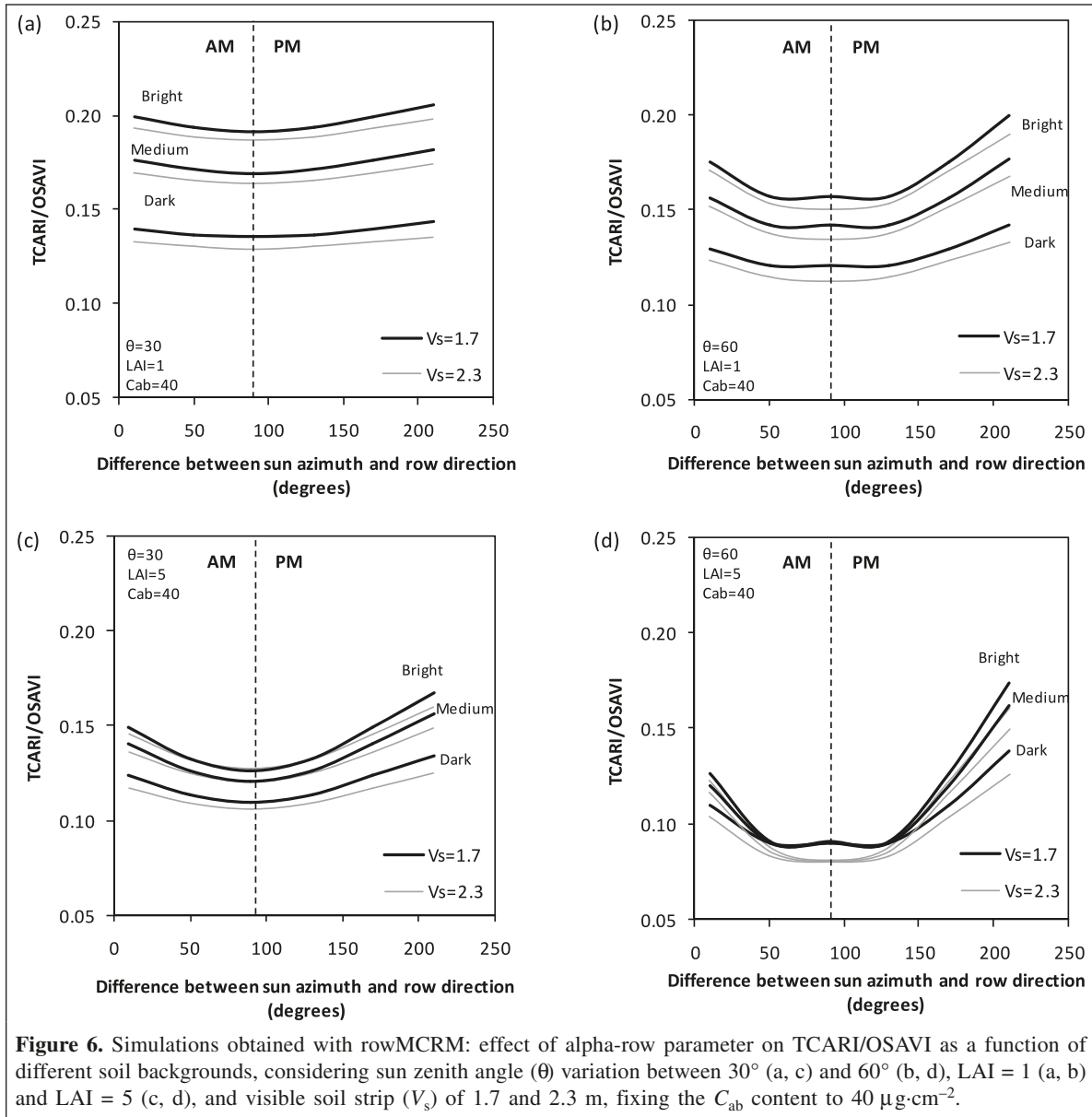


Figure 6. Simulations obtained with rowMCRM: effect of alpha-row parameter on TCARI/OSAVI as a function of different soil backgrounds, considering sun zenith angle (θ) variation between 30° (a, c) and 60° (b, d), LAI = 1 (a, b) and LAI = 5 (c, d), and visible soil strip (V_s) of 1.7 and 2.3 m, fixing the C_{ab} content to $40 \mu\text{g}\cdot\text{cm}^{-2}$.

dataset where a larger RMSE of $20.3 \mu\text{g}\cdot\text{cm}^{-2}$ was observed (Figure 9b). This result underscores the importance of considering the viewing geometry and row orientation effects on canopy BRDF. In this study, two new algorithms were calculated specifically for an AM and PM viewing geometry (Table 2; Equations (3) and (4)), which yielded good results with an RMSE of 8.6 and $10.8 \mu\text{g}\cdot\text{cm}^{-2}$ for the AM and PM datasets, respectively (Figure 9c). Furthermore, a unique comprehensive new algorithm for both AM and PM viewing geometries (Table 2; Equation (5)) was generated based on simulations accounting for daily BRDF variations in viewing geometries and row orientations. In this case, the rowMCRM was used to estimate the changes in the computed TCARI/OSAVI corresponding to changes in sun geometry and row orientation to apply the new upscaling algorithm (Equation (5)) to estimate leaf C_{ab} . This predictive relationship yielded

good results from both AM and PM datasets, with an RMSE of 10.2 and $10.6 \mu\text{g}\cdot\text{cm}^{-2}$, respectively (Figure 9d).

Hyperspectral CASI images collected in spectral mode (at a resolution at which pixels are aggregated soil-vegetation) of the different study sites (Figure 10, left) were computed using the new unique predictive relationship proposed in this study and displayed in Figure 10 (Table 2; Equation (5)). This algorithm proposed for the upscaling of TCARI/OSAVI to estimate the C_{ab} content, considering both AM and PM viewing geometries and the differences in vine row orientation, was applied to the CASI images to obtain maps of leaf C_{ab} content for five classes of concentration, from 5 to $80 \mu\text{g}\cdot\text{cm}^{-2}$. The within-field spatial variation of C_{ab} content is observed (Figure 10a) due to soil composition and nutrition differences. Examples of fields having high (Figure 10b), medium (Figure 10c), and low (Figure 10d) C_{ab} content ($\mu\text{g}\cdot\text{cm}^{-2}$) are

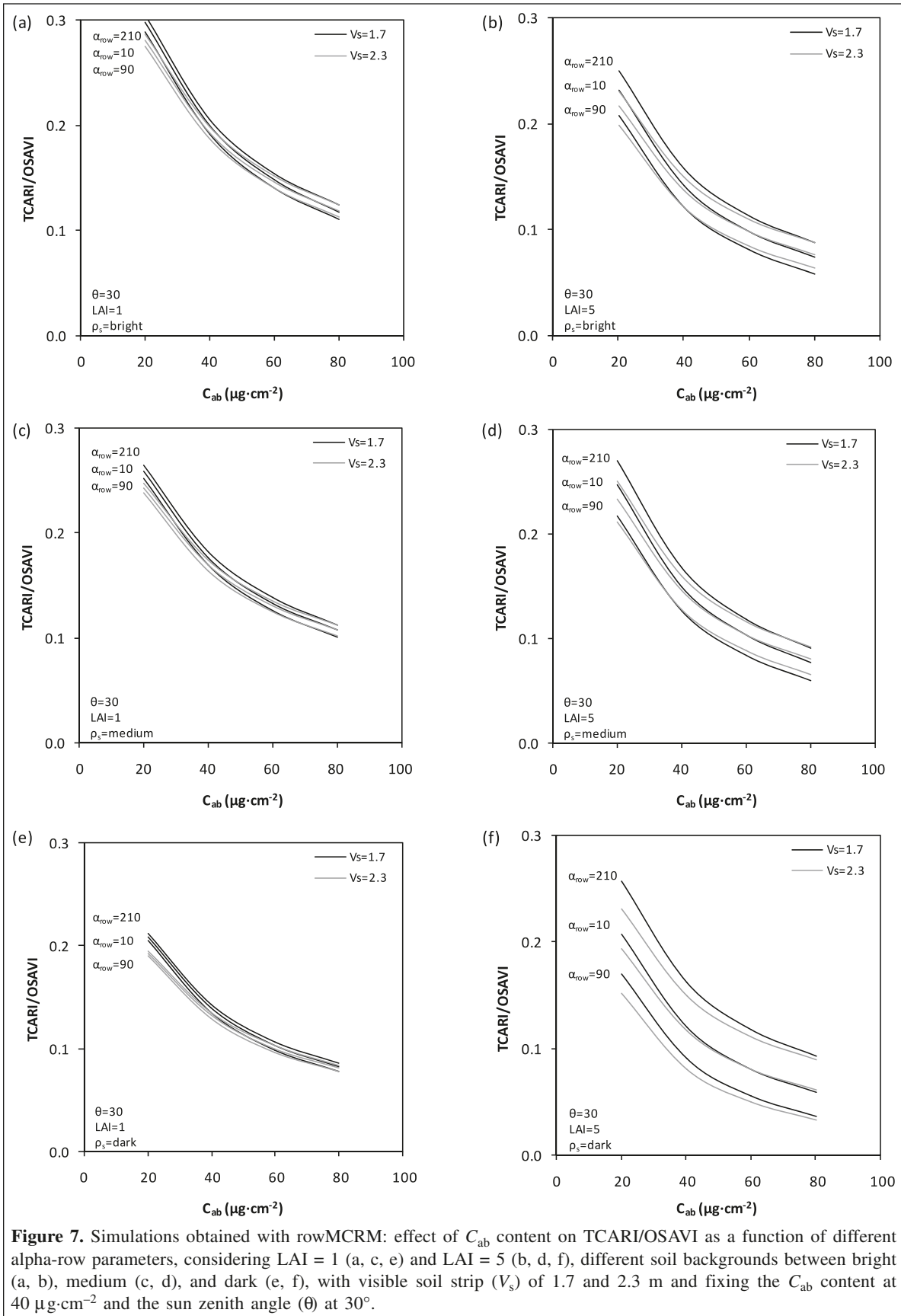


Figure 7. Simulations obtained with rowMCRM: effect of C_{ab} content on TCARI/OSAVI as a function of different alpha-row parameters, considering LAI = 1 (a, c, e) and LAI = 5 (b, d, f), different soil backgrounds between bright (a, b), medium (c, d), and dark (e, f), with visible soil strip (V_s) of 1.7 and 2.3 m and fixing the C_{ab} content at $40 \mu\text{g}\cdot\text{cm}^{-2}$ and the sun zenith angle (θ) at 30° .

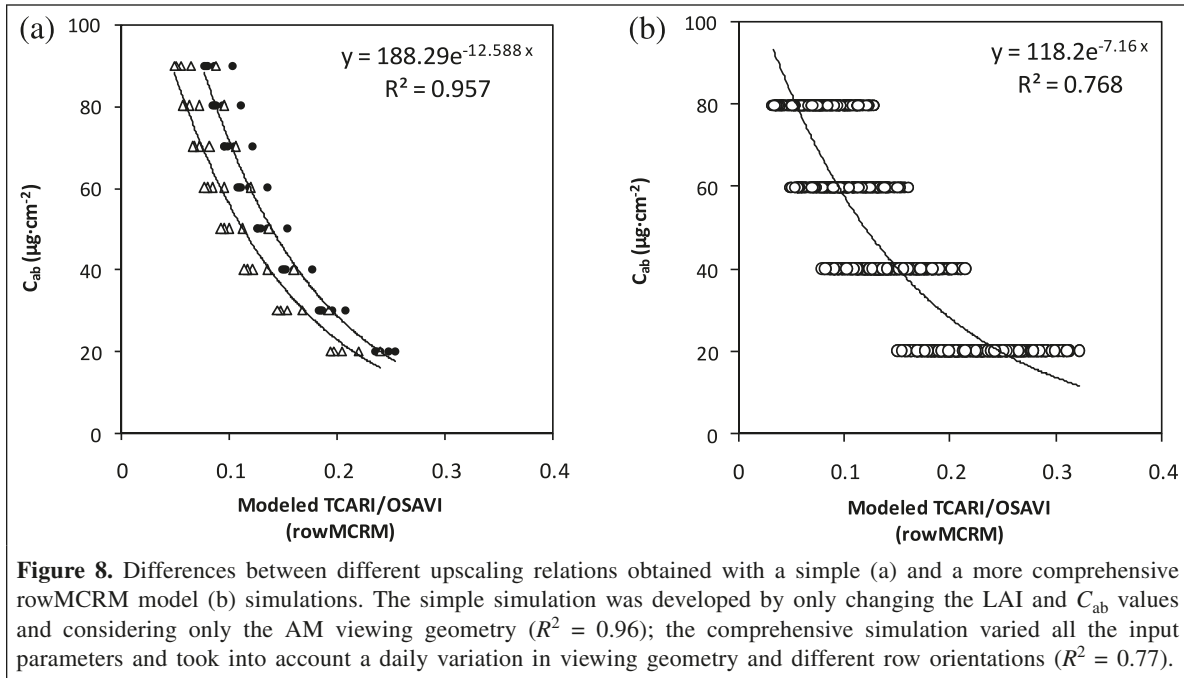


Figure 8. Differences between different upscaling relations obtained with a simple (a) and a more comprehensive rowMCRM model (b) simulations. The simple simulation was developed by only changing the LAI and C_{ab} values and considering only the AM viewing geometry ($R^2 = 0.96$); the comprehensive simulation varied all the input parameters and took into account a daily variation in viewing geometry and different row orientations ($R^2 = 0.77$).

Table 2. Summary of results obtained among predictive algorithms for C_{ab} estimation (y) through the upscaling of modelled TCARI/OSAVI (x).

Equation	Equation No.	RMSE ($\mu\text{g}\cdot\text{cm}^{-2}$)		
		Spatial mode (AM)	Spectral mode (PM)	
Test of predictive upscaling relations taken from literature				
Haboudane et al. (2002)	$y = -30.194 \ln(x) - 18.363$	(1)	41.2	32.9
Zarco-Tejada et al. (2005)	$y = 188.29 \exp[-12.588(x)]$	(2)	11.2	20.3
New algorithms obtained from modelled TCARI/OSAVI with rowMCRM to assess BRDF and row orientation effects				
Equation obtained for AM geometries	$y = 125.2 \exp[-8.46(x)]$	(3)	8.6	14.2
Equation obtained for PM geometries	$y = 149.8 \exp[-8.19(x)]$	(4)	14.3	10.8
Results using Equations (3) and (4) for AM and PM datasets, respectively		(3) + (4)	8.6	10.8
Unique upscaling relation considering BRDF and row orientation effects	$y = 118.2 \exp[-7.16(x)]$	(5)	10.2	10.6

presented. The accuracy of these C_{ab} spatial variation maps calculated from the CASI images in spectral mode is considered consistent with the $10.6 \mu\text{g}\cdot\text{cm}^{-2}$ RMSE retrieval accuracy expected.

Conclusions

This study investigated the effect of different sun viewing geometries and row orientations on the canopy reflectance for leaf chlorophyll content estimation, taking into consideration the complex discontinuous structure typical of vineyards. Airborne campaigns imaged a total of 72 study sites from 14 vineyard fields with the CASI hyperspectral sensor.

To assess the BRDF effects on canopy reflectance, caused by different shadow fractions from variable sun viewing geometries and row orientations, the two airborne CASI mission datasets

were collected over the same sites in the morning (1 m spatial mode) and in the afternoon (4 m spectral mode). Spectra (mixed pixels of vegetation and soil) extracted for specific study sites from the CASI images showed an offset between the two datasets (AM and PM) that was also evident in the calculated indices (TCARI/OSAVI, NDVI) for the same sites.

To understand the role of different sun viewing geometries coupled with different row orientations of the canopy reflectance observed from the CASI images, the rowMCRM was used for simulation of expected reflectance spectra from these open-row canopies. This model takes into account row orientation and canopy structure (vine width, visible soil strip, row LAI) and different sun viewing geometries. Simulations were conducted with the rowMCRM canopy model to understand the behavior of the alpha-row parameter, the angular difference between the sun azimuth angle and the row

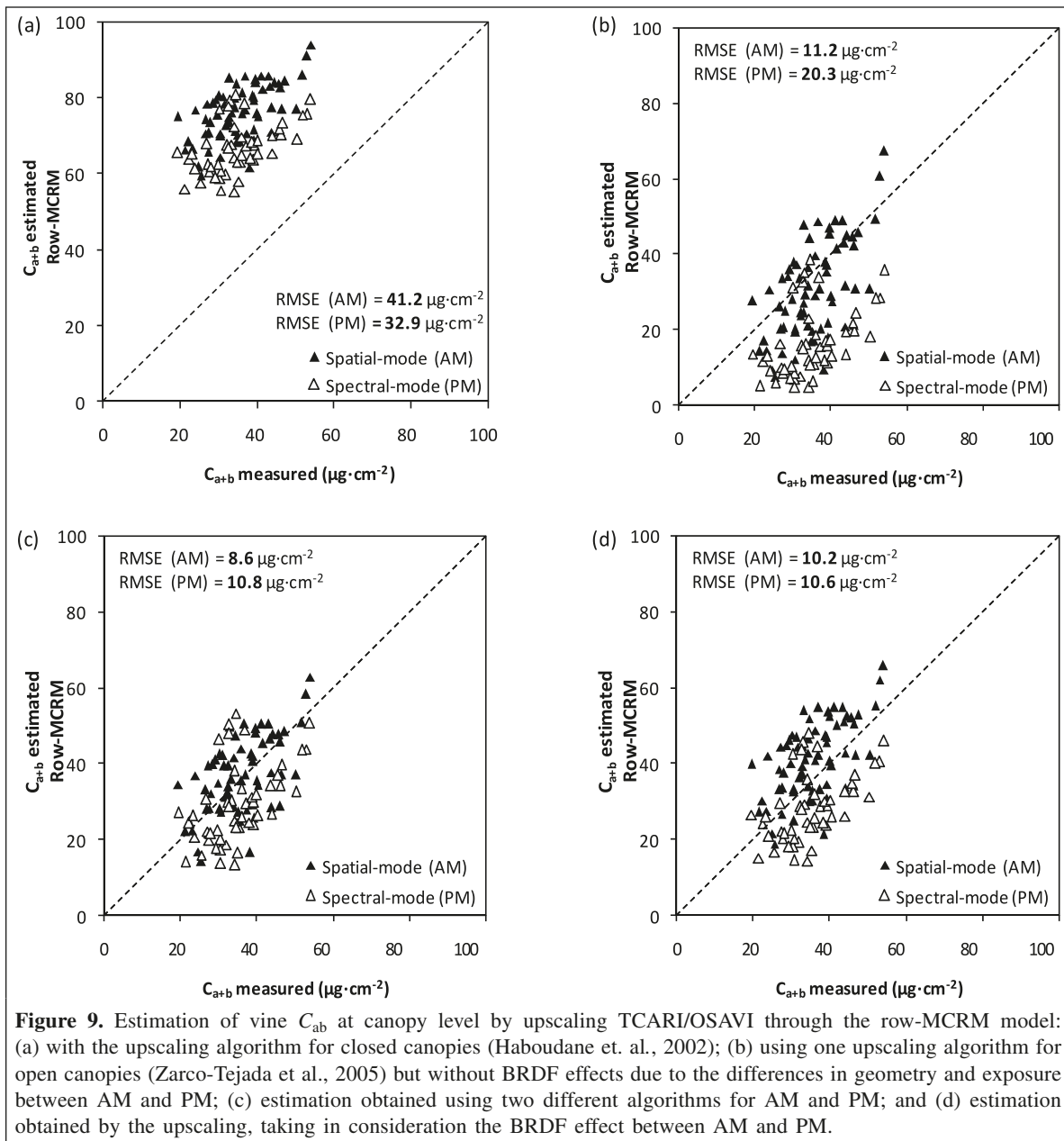
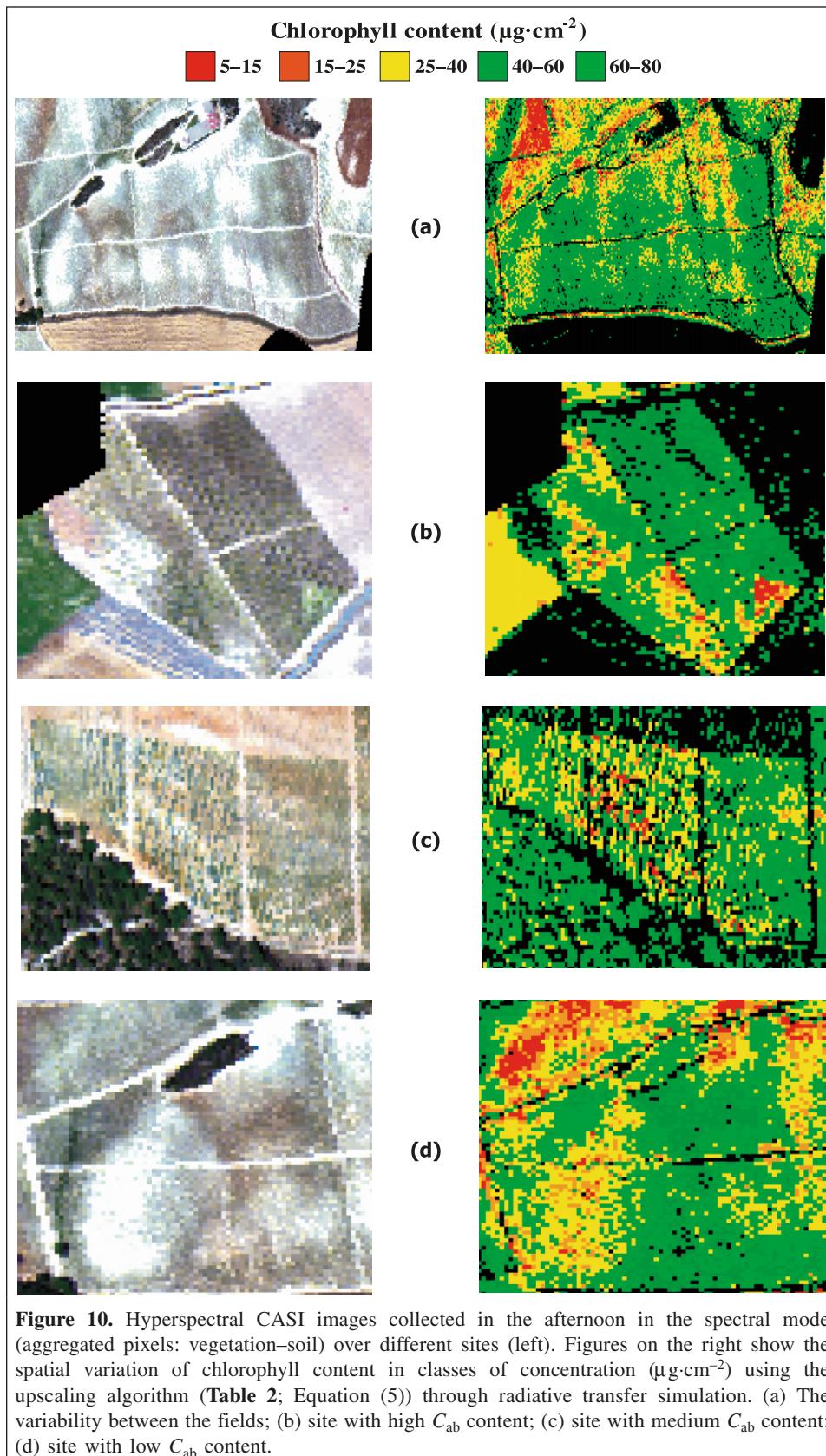


Figure 9. Estimation of vine C_{ab} at canopy level by upscaling TCARI/OSAVI through the row-MCRM model: (a) with the upscaling algorithm for closed canopies (Haboudane et al., 2002); (b) using one upscaling algorithm for open canopies (Zarco-Tejada et al., 2005) but without BRDF effects due to the differences in geometry and exposure between AM and PM; (c) estimation obtained using two different algorithms for AM and PM; and (d) estimation obtained by the upscaling, taking in consideration the BRDF effect between AM and PM.

orientation, both calculated from north in a clockwise direction. A previous paper (Zarco-Tejada et al., 2005) assessed the effect of different structural parameters (e.g., vine height, vine width, visible soil strip, and LAI) of the canopy reflectance using this model. That paper emphasized the use of simulations with the rowMCRM to understand the effect of the alpha-row parameter on the estimation of leaf chlorophyll content. In particular, the effect of the alpha-row parameter was considered as a function of daily variations of the sun viewing geometry (zenith and azimuth angles) and of different canopy structures, soil backgrounds, and chlorophyll content. The simulations confirmed that viewing geometry and row orientation are the major drivers of the variation in canopy reflectance observed between the CASI datasets. Consequently, it is imperative to take into account BRDF effects from shadows in the canopy

pixels during the day in the planning of a field campaign. In particular, the simulations underscored the value of the central part of the day as the best time to collect images, since shadows are reduced when the sun zenith angle is around 10° . Canopy R was most influenced by row LAI and soil background, such that the viewing geometry and row orientation effects were reduced in the central part of the day. A different range in sun zenith angles and alpha-row parameters enabled minimizing BRDF effects on the TCARI/OSAVI index used to estimate C_{ab} .

Simulations conducted in this study with the rowMCRM canopy model enabled the calculation of different predictive relationships, considering ranges of all the parameters describing leaf, canopy structure, and soil background properties and sun-sensor geometry. Different predictive algorithms were tested in this study to explore the importance



of row orientation and viewing geometry of row-structured crops. Predictive relationships from the literature (Zarco-Tejada et al., 2005; Haboudane et al., 2002) were compared with new predictive relationships developed in this study. The results obtained using the predictive relationship proposed by Haboudane et al. (2002) for corn closed canopies showed an overestimation of C_{ab} concentration with an RMSE of 41.2 and 32.9 $\mu\text{g}\cdot\text{cm}^{-2}$ for morning and afternoon datasets, respectively. These results emphasize, as expected, the need to use an open-canopy upscaling relationship for row-structured canopies. The relationship proposed by Zarco-Tejada et al. (2005) for open canopies, but obtained only considering the AM viewing geometry, yielded a much improved RMSE of 11.2 $\mu\text{g}\cdot\text{cm}^{-2}$ for the AM dataset, as previously reported; nevertheless, for the PM dataset, a significantly larger RMSE of 20.3 $\mu\text{g}\cdot\text{cm}^{-2}$ was found. This result underscores the importance of considering the viewing geometry and row orientation effect on canopy reflectance due to BRDF changes. A new unique algorithm applicable to both morning and afternoon viewing geometries proposed in this study, based on comprehensive simulation results, yielded good results from both datasets with an RMSE of 10.2 and 10.6 $\mu\text{g}\cdot\text{cm}^{-2}$, respectively. This new unique algorithm avoids the need for two different relationships specific for the morning and afternoon viewing geometries (RMSE of 8.6 and 10.8 $\mu\text{g}\cdot\text{cm}^{-2}$, respectively) without compromising prediction accuracy.

These results suggest the importance of taking into account the spatial and temporal variability of the BRDF effects due to the diurnal differences in the viewing geometries and row orientation in the use of hyperspectral remote sensing data, to accurately estimate leaf chlorophyll content. The planning of multispectral and hyperspectral flight campaigns must take into consideration this variability to minimize the BRDF effect and to obtain accurate canopy reflectance datasets, and thus estimate leaf chlorophyll content with greater precision.

Acknowledgements

Financial supports from the Spanish Ministry of Education (MEC) for the project AGL2005-04049 and from the Natural Sciences and Engineering Research Council (NSERC) of Canada to permit contributions by J.R. Miller are gratefully acknowledged. F. Meggio is supported by the FISIR Project CarboItaly and gratefully acknowledges the financial support from the Gini Foundation. The authors are grateful to Consejo Regulador de la Denominación de Origen Ribera de Duero, Bodegas Monasterio S.L., and Fertiberia S.A. for their collaboration to conduct this research. We thank L. Gray and J. Freemantle from York University, and the Instituto Nacional de Técnica Aeroespacial (INTA) Remote Sensing Laboratory for efficient airborne campaigns with the CASI sensor, providing coordination with field data collection. A. Kuusk and J. Praks are gratefully acknowledged for sharing the rowMCRM code, and R. Lopez for programming assistance with the radiative transfer models.

References

- Ben-Dor, E., and Levin, N. 2000. Determination of surface reflectance from raw hyperspectral data without simultaneous ground data measurements: a case study of the GER 63-channel sensor data acquired over Naan, Israel. *International Journal of Remote Sensing*, Vol. 21, pp. 2053–2074.
- Carter, G.A. 1994. Ratios of leaf reflectances in narrow wavebands as indicators of plant stress. *International Journal of Remote Sensing*, Vol. 15, pp. 697–704.
- Daughtry, C.S.T., Walthall, C.L., Kim, M.S., Brown de Colstoun, E., and McMurtry, III., J.E. 2000. Estimating corn leaf chlorophyll concentration from leaf and canopy reflectance. *Remote Sensing of Environment*, Vol. 74, pp. 229–239.
- Gitelson, A.A., and Merzlyak, M.N. 1996. Signature analysis of leaf reflectance spectra: algorithm development for remote sensing of chlorophyll. *Journal of Plant Physiology*, Vol. 148, pp. 494–500.
- Haboudane, D., Miller, J.R., Tremblay, N., Zarco-Tejada, P.J., and Dextraze, L. 2002. Integration of hyperspectral vegetation indices for prediction of crop chlorophyll content for application to precision agriculture. *Remote Sensing of Environment*, Vol. 81, Nos. 2–3, pp. 416–426.
- Haboudane, D., Miller, J.R., Pattey, E., Zarco-Tejada, P.J., and Strachan, I. 2004. Hyperspectral vegetation indices and novel algorithms for predicting green LAI of crop canopies: modeling and validation in the context of precision agriculture. *Remote Sensing of Environment*, Vol. 90, No. 3, pp. 337–352.
- Hall, A., Lamb, D.W., Holzapfel, B., and Louis, J. 2002. Optical remote sensing applications in viticulture—a review. *Australian Journal of Grape and Wine Research*, Vol. 8, No. 1, pp. 36–47.
- Hall, A., Louis, J., and Lamb, D. 2003. Characterising and mapping vineyard canopy using high-spatial-resolution aerial multispectral images. *Computers and Geosciences*, Vol. 29, pp. 813–822.
- Johnson, L.F., Bosch, D.F., Williams, D.C., and Lobitz, B.M. 2001. Remote sensing of vineyard management zones: implications for wine quality. *Applied Engineering in Agriculture*, Vol. 17, No. 4, pp. 557–560.
- Kuusk, A. 1995a. A fast, invertible canopy reflectance model. *Remote Sensing of Environment*, Vol. 51, pp. 342–350.
- Kuusk, A. 1995b. A Markov chain model of canopy reflectance. *Agricultural and Forest Meteorology*, Vol. 76, pp. 221–236.
- Martin, P., Zarco-Tejada, P.J., Gonzalez, M.R., and Berjón, A. 2007. Using hyperspectral remote sensing to map grape quality in “Tempranillo” vineyards affected by iron deficiency chlorosis. *Vitis*, Vol. 46, No. 1, pp. 7–14.
- O’Neill, N.T., Zagolski, F., Bergeron, M., Royer, A., Miller, J.R., and Freemantle, J. 1997. Atmospheric correction validation of CASI images acquired over the BOREAS southern study area. *Canadian Journal of Remote Sensing*, Vol. 23, pp. 143–162.
- Rock, B.N., Hoshizaki, T., and Miller, J.R. 1988. Comparison of in situ and airborne spectral measurements of the blue shift associated with forest decline. *Remote Sensing of Environment*, Vol. 24, pp. 109–127.
- Rondeaux, G., Steven, M., and Baret, F. 1996. Optimization of soil-adjusted vegetation indices. *Remote Sensing of Environment*, Vol. 55, pp. 95–107.
- Vogelmann, J.E., Rock, B.N., and Moss, D.M. 1993. Red edge spectral measurements from sugar maple leaves. *International Journal of Remote Sensing*, Vol. 14, pp. 1563–1575.

- Zarco-Tejada, P.J., Miller, J.R., Mohammed, G.H., Noland, T.L., and Sampson, P.H. 2001. Scaling-up and model inversion methods with narrow-band optical indices for chlorophyll content estimation in closed forest canopies with hyperspectral data. *IEEE Transactions on Geoscience and Remote Sensing*, Vol. 39, No. 7, pp. 1491– 1507.
- Zarco-Tejada, P.J., Berjón, A., Morales, A., Miller, J.R., Agüera, J., and Cachorro, V. 2003. Leaf biochemistry estimation on EU high-value crops with ROSIS and DAIS hyperspectral data and radiative transfer simulation. *3rd EARSeL Workshop on Imaging Spectroscopy*. Germany, Munich. pp. 597–602.
- Zarco-Tejada, P.J., Miller, J.R., Morales, A., Berjón, A., and Agüera, J. 2004. Hyperspectral indices and model simulation for chlorophyll estimation in open-canopy tree crops. *Remote Sensing of Environment*, Vol. 90, No. 4, pp. 463–476.
- Zarco-Tejada, P.J., Berjón, A., Lopez-Lozano, R., Miller, J.R., Martin, P., Cachorro, V., et al. 2005. Assessing vineyard condition with hyperspectral indices: leaf and canopy reflectance simulation in a row-structured discontinuous canopy. *Remote Sensing of Environment*, Vol. 99, pp. 271– 287.